05

Shape memory effect of the Fe−16Mn−10Cr−8Ni−4Si alloy single crystals under tension

© I.V. Kireeva, Yu.I. Chumlyakov, A.V. Fedorova, I.V. Kuksgauzen, D.A. Kuksgauzen

Tomsk State University, Tomsk, Russia
E-mail: kireeva@spti.tsu.ru

Received July 8, 2025
Revised August 12, 2025
Accepted August 12, 2025

For the first time, in the Fe−16Mn−10Cr−8Ni−4Si (wt.%) alloy single crystals with a reversible FCC↔HCP martensitic transformation (MT), oriented for tension along the $[\bar{1}11]$ direction, a shape memory effect (SME) of 10 % was obtained with a successive increase in strain in the „load-unloading"cycle and heating in a free state. The magnitude of the SME turned out to be close to the theoretical value of the transformation strain $\varepsilon_{tr} = 10.8\,\%$ for FCC−HCP MT in this orientation under tension. The physical reason for achieving the SME close to the theoretical value of ε_{tr} is associated with a high level of stresses at the yield point $\sigma_{0.1}$ of the initial FCC phase, which leads to the development of FCC↔HCP MT under stress without defect formation.

Keywords: single crystals, FCC−HCP martensitic transformation, shape memory effect, tension

DOI: 10.61011/TPL.2025.11.62212.20434

The interest in iron-based Fe−Mn−Cr−Ni−Si alloys with a shape memory effect (SME) associated with a reversible FCC↔HCP martensitic transformation (MT) has been on the rise in the last decade [1–4]. These alloys have cheap components, a disordered structure, and high plasticity in austenite, which allows for the use of well-developed methods for their smelting and production of articles for commercial goods [1,3]. In terms of the SME magnitude, these alloys are on par with those based on Ti−Ni. An SME magnitude up to 7.6 % [1] was obtained in polycrystals of the Fe−20.2Mn−5.6Si−8.9Cr−5.0Ni (wt.%) alloy after casting without any additional thermomechanical treatment. The maximum SME associated with the FCC−HCP MT in single crystals of the Fe−30Mn−1Si alloy was 8−9.2 % under tensile strain in the $[\bar{1}44]$ orientation, while the maximum value of transformation strain ε_{tr} for the FCC−HCP MT in this orientation under tension is 17.5 % [5,6]. An SME associated with the FCC−HCP MT equal in magnitude to the theoretical value of the transformation strain has not been reported to date in studies of iron-based Fe−Mn−Si alloys. There are several physical reasons why theoretical values of ε_{tr} were not achieved experimentally in iron-based Fe−Mn−Si alloys: (1) interaction of HCP-martensite variants suppresses the reversible motion of martensite crystal boundaries upon heating; (2) the volume fraction of forming BCT-martensite increases with decreasing temperature, which has a negative effect on shape memory; (3) low strength properties of the initial FCC phase facilitate the development of plastic deformation through slip or twinning during the FCC↔HCP MT [1,4–6].

In the present study, we report the results of examination of SME associated with the FCC↔HCP MT in single crystals of the Fe−16Mn−10Cr−8Ni−4Si (wt.%) alloy oriented for tension along the $[\bar{1}11]$ direction. Crystals with tension axis $[\bar{1}11]$ are oriented for multiway development of HCP-martensite variants from the onset of deformation. The theoretical transformation strain for this orientation under tension is $\varepsilon_{tr} = Sm = 10.8\,\%$ ($S = 0.35$ is the shift under the FCC−HCP MT and $m = 0.31$ is the Schmid factor for the formation of monovariant HCP-martensite) [7,8]. This orientation allows us to investigate the magnitude of SME under the condition of interaction of HCP-martensite variants from the onset of deformation.

Single crystals of the Fe−16Mn−10Cr−8Ni−4Si alloy were grown by the Bridgman method in a helium atmosphere. Their orientation was determined using a DRON-3M diffractometer and FeK_α. Dumb-bell samples $2 \times 1.5 \times 15$ mm in size were cut out using an electrospark discharge machine. Samples were homogenized in helium at 1373 K for 14 h and quenched in water. Temperatures $M_s = 195 \pm 3$ K, $M_f = 138 \pm 3$ K corresponding to the start and finish of the forward MT under cooling and $A_s = 295 \pm 3$ K, $A_f = 340 \pm 3$ K corresponding to the start and finish of the reverse MT under heating were determined from the temperature dependence of electrical resistivity $\rho(T)$. The temperature dependence of yield point $\sigma_{0.1}(T)$, stress−strain curves, and the SME under a constant temperature ($M_s = 195$ and 77 K) and increasing strain in the load−unload cycle were investigated using an Instron 5969 testing system at a strain rate of $4 \cdot 10^{-4}\,\mathrm{s}^{-1}$. Dependence $\sigma_{0.1}(T)$ was examined for a single sample at temperatures ranging first from 300 to 523 K and then from 300 to 77 K. In order to reduce the influence of plastic deformation on $\sigma_{0.1}$ within the next temperature range, the sample was deformed to a residual strain of 0.1 %. Electron microscopic studies were carried out using a Jeol 2010 microscope at an accelerating voltage of 200 kV.

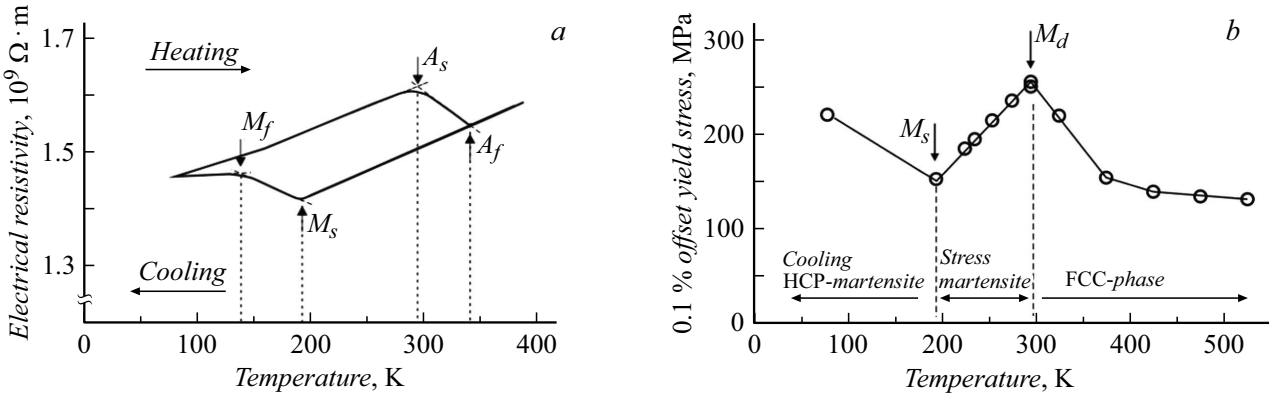

Figure 1. Temperature dependence of electrical resistivity $\rho(T)$ (a) and yield point $\sigma_{0.1}(T)$ under tension (b) of $[\bar{1}11]$ single crystals of the Fe−16Mn−10Cr−8Ni−4Si alloy with a reversible FCC↔HCP MT.

The temperature dependence of electrical resistivity $\rho(T)$ examined under cooling to 77 K and heating to 400 K reveals a closed loop (Fig. 1, a) characteristic of the reversible MT [7,8]. The FCC↔HCP MT develops in single crystals of the Fe−16Mn−10Cr−8Ni−4Si alloy under cooling/heating in a free state within a wide temperature interval and is characterized by thermal hysteresis $\Delta T_h = A_f - M_s = 145$ K (Fig. 1, a). A typical MT dependence is not observed in the $\rho(T)$ curve under cooling and heating in alloys of the Fe−Mn−Si system if $T_N > M_s$ (T_N is the Néel temperature at which the FCC phase goes from a paramagnetic state to an antiferromagnetic one) [9]. Therefore, temperature T_N in single crystals of Fe−16Mn−10Cr−8Ni−4Si is below the liquid nitrogen temperature and does not affect the formation of cooling HCP-martensite [10].

The temperature dependence of yield point $\sigma_{0.1}(T)$ within the temperature range of 77–523 K consists of three stages that are observed in alloys undergoing MT under load [7,8] (Fig. 1, b). A joint analysis of the $\rho(T)$ and $\sigma_{0.1}(T)$ dependences reveals that minimum stress $\sigma_{0.1} = 150 \pm 10$ MPa in the $\sigma_{0.1}(T)$ dependence corresponds to temperature $M_s = 195 \pm 3$ K [7,8]. At $T < M_s$, stresses $\sigma_{0.1}$ increase with decreasing temperature, and $\alpha = d\sigma_{0.1}/dT$ is negative. This stage in the $\sigma_{0.1}(T)$ dependence is associated with the onset of deformation of cooling HCP-martensite. At $T = 300$ K, dependence $\sigma_{0.1}(T)$ has a maximum $\sigma_{0.1} = 255 \pm 10$ MPa. This temperature corresponds to temperature M_d at which the stresses for the onset of formation of stress HCP-martensite (SM) and for the onset of plastic deformation of the initial phase are equal [7,8]. An anomalous temperature dependence is found within the $M_s - M_d$ interval, where stresses $\sigma_{0.1}$ increase with temperature, $\sigma = d\sigma_{0.1}/dT > 0$, and dependence $\sigma_{0.1}(T)$ follows the Clausius−Clapeyron relation [7,8]:

$$\alpha = \frac{d\sigma_{0.1}(T)}{dT} = -\frac{\Delta S}{\varepsilon_{tr}} = -\frac{\Delta H}{T_0 \varepsilon_{tr}} > 0. \qquad (1)$$

Here, ΔS and ΔH are the changes in entropy and enthalpy during MT per unit volume, respectively; ε_{tr} is the transformation strain for the FCC−HCP transformation, and T_0 is the temperature of chemical equilibrium of phases. The temperature interval for SM is 102 ± 5 K, and $\alpha = d\sigma_{0.1}/dT = 1.02$ MPa/K. At $T > M_d$, stresses $\sigma_{0.1}$ decrease and $\alpha = d\sigma_{0.1}/dT$ becomes negative. This stage is associated with the onset of plastic deformation of the FCC phase [7,8].

Electron microscopic studies reveal in $[\bar{1}11]$ single crystals formation of HCP-martensite right from the start at a temperature $T \leqslant M_s$ (Fig. 2), which is reversible, and the SME takes place. The shape memory effect was studied at a constant temperature (77 K and $T = M_s = 195$ K) with a sequential increase in strain in the load-unload cycle and subsequent heating in a free state. The sample was heated in two ways: in a dilatometer until the completion of the reverse HCP−FCC transition and in a furnace at a temperature of 573 K for 15 min. In each case, the

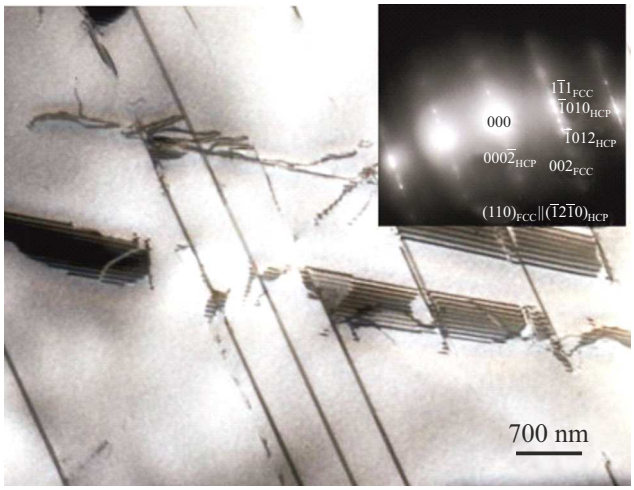

Figure 2. HCP-martensite in $[\bar{1}11]$ single crystals of the Fe−16Mn−10Cr−8Ni−4Si alloy after tensile strain (5%) at temperature $M_s = 195$ K.

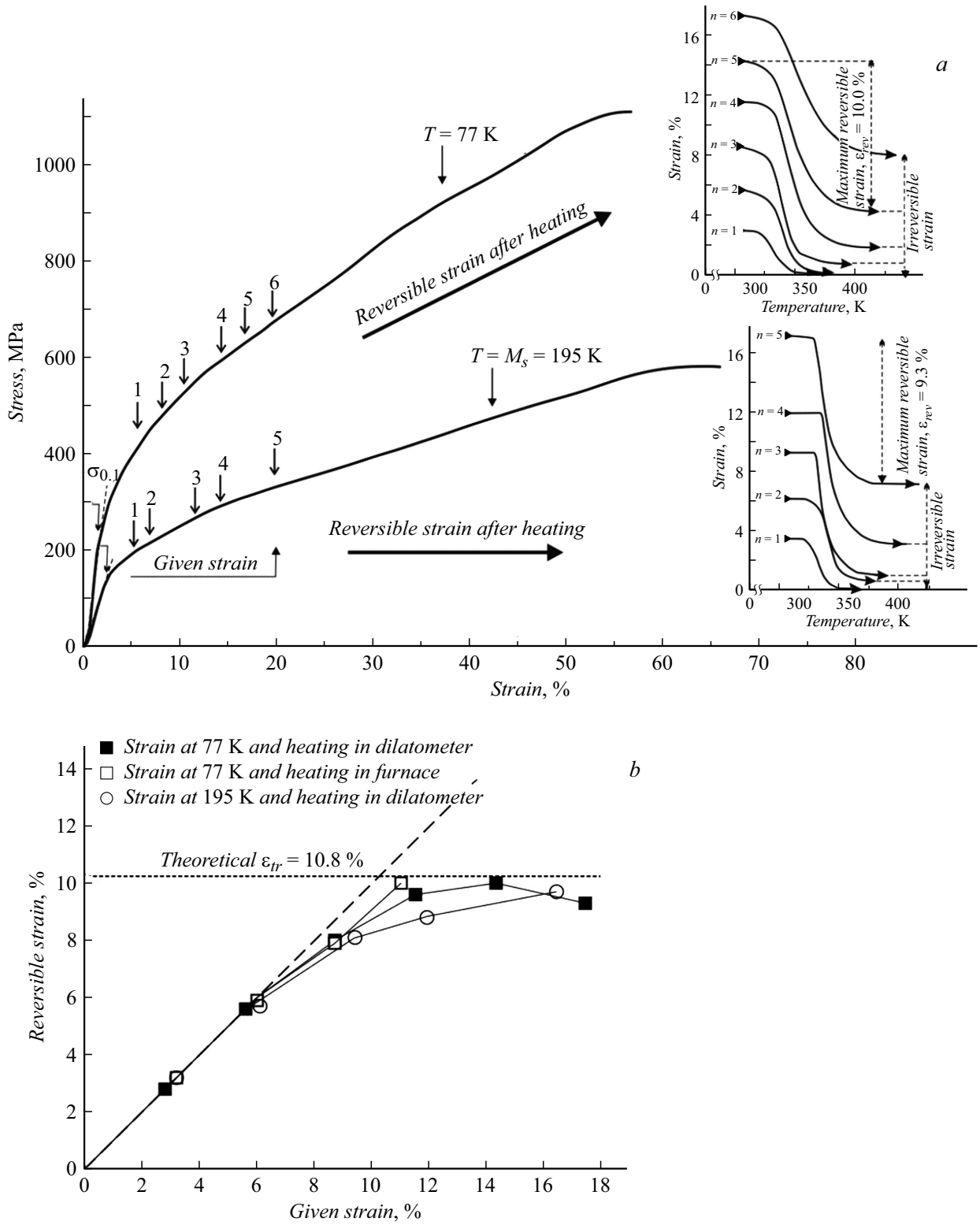

Figure 3. Stress–strain curves and corresponding strain–temperature curves after heating in the dilatometer following prestrain in the load-unload cycle (*a*) and reversible strain (*b*) of [$\bar{1}$11] single crystals of the Fe–16Mn–10Cr–8Ni–4Si alloy. The numbers next to stress–strain curves indicate prestrain in the load-unload cycle.

subsequent strain was increased after heating. Since the strain in each new load-unload cycle after heating was increased in experiments with the same sample, this may be regarded as aging.

The complete stress–strain curves at 77 and 195 K are shown in Fig. 3, *a*. The numbers next to the curves indicate the magnitude of prestrain in the load-unload cycle. According to the $\rho(T)$ dependence (Fig. 1, *a*), the stress–strain curve is shaped by the deformation of cooling HCP-martensite at a temperature of 77 K and by the deformation of stress martensite at 195 K [7,8]. It can be seen from Fig. 3 that reversible strain $\varepsilon_{rev} = \varepsilon_{shme}$ (*shme* — shape memory effect) after heating increases linearly with increasing strain in the load-unload cycle. The results of two types of SME measurements match. At 77 K, the maximum SME of 10 % was obtained after a prestrain of 14.4 and 11 % in the load-unload cycle with heating in the dilatometer and in the furnace, respectively (Fig. 3, *b*). At a temperature of 195 K, the maximum SME of 9.3 % was obtained after a prestrain of 16.4 % in the load-unload cycle with heating in the dilatometer. At 77 K, the SME was found to be close to the theoretical value of transformation strain $\varepsilon_{tr} = 10.8\,\%$ for the FCC–HCP MT under tension for the $[\bar{1}11]$ orientation [7] and greater than the maximum SME of 8–9.2 % in the $[\bar{1}44]$ orientation of the Fe–30Mn–1Si alloy [5,6]. An SME of 7.4 and 6.8 % close theoretical value $\varepsilon_{tr} = 10.8\,\%$ for the FCC–HCP MT under tension for the $[\bar{1}11]$ orientation has been obtained earlier in $[\bar{1}11]$ single crystals of the high-entropy $Cr_{20}Mn_{20}Fe_{20}Co_{35}Ni_5$ alloy with the FCC↔HCP MT under similar deformation conditions [11].

A joint analysis of data presented here and earlier in [5,6,11] demonstrates, first, that the substitution of Mn atoms in the Fe–30Mn–1Si alloy by Cr and Ni atoms leads to significant strengthening of the initial FCC phase in Fe–16Mn–10Cr–8Ni–4Si single crystals. At temperature M_d, stresses $\sigma_{0.1}(M_d) = 255 \pm 10$ MPa in the studied Fe–16Mn–10Cr–8Ni–4Si single crystals are 3.5 times higher than $\sigma_{0.1}(M_d) = 70–75$ MPa in Fe–30Mn–1Si single crystals [5,6]. Owing to this, the development of several variants of HCP-martensite in $[\bar{1}11]$ single crystals right from the start of deformation and their interaction with each other under load occur without defect formation, which is accompanied by an enhancement of SME, as was demonstrated earlier in solid-solution strengthening of single crystals of the high-entropy $(FeMnCr)_{60}Co_{35}Ni_{4.8}C_{0.2}$ alloy by carbon atoms [12]. Second, doping with Cr atoms enhances the short-range order (SRO) in Fe–16Mn–10Cr–8Ni–4Si single crystals. SRO hinders the formation of large plates of HCP-martensite during growth in thickness, since this SRO needs to be disrupted by partial Shockley dislocations $a/6\langle 112\rangle$ through one plane $\{111\}$. In the case of forward MT under load, thin HCP-martensite does not produce intense stress concentrations at the head of a martensite plate, which are accommodated elastically without plastic deformation of the initial phase. When the load is removed, it reverts „exactly“ back after heating [12]. Third, when the strain is increased in load-unload cycles at 77 K, BCT-martensite emerges in $[\bar{1}11]$ Fe–16Mn–10Cr–8Ni–4Si single crystals after 5 % strain at the points of intersection of HCP-martensite variants with each other and does not exert a negative influence on the SME due to the smallness of its volume fraction [4].

Superelasticity does not emerge in $[\bar{1}11]$ Fe–16Mn–10Cr–8Ni–4Si single crystals during the FCC–HCP MT under load within the $M_s–M_d$ temperature range. First, the FCC↔HCP MT is characterized by a broad thermal hysteresis $\Delta T_h = 145$ K; second, temperature A_f in these crystals is higher than temperature M_d (Fig. 1). This implies that the thermodynamic conditions for superelasticity are not established in $[\bar{1}11]$ Fe–16Mn–10Cr–8Ni–4Si single crystals [7,8].

Thus, a reversible FCC↔HCP MT with thermal hysteresis $\Delta T_h = A_f – M_s = 145$ K develops in $[\bar{1}11]$ single crystals of the Fe–16Mn–10Cr–8Ni–4Si (wt.%) alloy. An SME of 10 % has been observed for the first time for the FCC↔HCP MT in the $[\bar{1}11]$ orientation at a temperature of 77 K under tension in the case of development of several HCP-martensite variants. This SME is close in magnitude to the theoretical value of transformation strain of 10.8 % for the FCC↔HCP MT in this orientation under a sequential increase in strain in the load-unload cycle and heating in a free state.

Funding

This study was supported by grant No. 25-19-00023 from the Russian Science Foundation (https://rscf.ru/project/25-19-00023/).

Conflict of interest

The authors declare that they have no conflict of interest.

References

[1] T. Sawaguchi, T. Maruyama, H. Otsuka, A. Kushibe, Y. Inoue, K. Tsuzaki, Mater. Trans., **57** (3), 283 (2016). DOI: 10.2320/matertrans.MB201510
[2] Y. Fu, J. Lu, G. Gao, H. Peng, Y. Wen, J. Alloys Compd., **1010**, 177148 (2025). DOI: 10.1016/j.jallcom.2024.177148
[3] A. Algamal, H. Abedi, U. Gandhi, O. Benafan, M. Elahinia, A. Qattawi, J. Alloys Compd., **1010**, 177068 (2025). DOI: 10.1016/j.jallcom.2024.177068
[4] J. Chen, H.B. Peng, Q. Yang, S.L. Wang, F. Song, Y.H. Wen, Mater. Sci. Eng. A, **677**, 133 (2016). DOI: 10.1016/j.msea.2016.09.006
[5] A. Sato, E. Chishima, Y. Yamaji, T. Mori, Acta Met., **32**, 539 (1984). DOI: 10.1016/0001-6160(84)90065-8
[6] A. Sato, E. Chishima, K. Soma, T. Mori, Acta Met., **30**, 1177 (1982). DOI: 10.1016/0001-6160(82)90011-6
[7] K. Otsuka, C.M. Wayman, *Shape memory materials* (Cambridge University Press, Cambridge, 1998).
[8] K. Otsuka, X. Ren, Prog. Mater. Sci., **50** (5), 135 (2005). DOI: 10.1016/j.pmatsci.2004.10.001

[9] J.H. Yang, H. Chen, C.W. Wayman, Met. Trans. A, **23**, 1439 (1992). DOI: 10.1007/BF02647327
[10] H. Otsuka, H. Yamada, T. Maruyama, H. Tanahashi, S. Matsuda, M. Murakami, ISIJ Int., **30** (8), 674 (1990). DOI: 10.2355/isijinternational.30.674
[11] I.V. Kireeva, Yu.I. Chumlyakov, A.A. Saraeva, A.V. Vyrodova, Z.V. Pobedennaya, Mater. Lett., **131**, 133461 (2023). DOI: 10.1016/j.matlet.2022.133461
[12] I.V. Kireeva, Yu.I. Chumlyakov, A.A. Saraeva, D.A. Kuksgauzen, Mater. Lett., **397**, 138851 (2025). DOI: 10.1016/j.matlet.2025.138851

Translated by D.Safin